Environmental Technology & Innovation 14 (2019) 100353

Contents lists available at ScienceDirect

Environmental Technology & Innovation

journal homepage: www.elsevier.com/locate/eti

A novel tri-metal composite incorporated polyacrylamide hybrid material for the removal of arsenate, chromate and fluoride from aqueous media

S.K.T. Thathsara [a], Asitha T. Cooray [a,c], Dilru R. Ratnaweera [a], Thilini Kuruwita Mudiyanselage [a,b,*]

[a] Department of Chemistry, University of Sri Jayewardenepura, Sri Lanka
[b] Center for Advanced Material Research, University of Sri Jayewardenepura, Sri Lanka
[c] Instrument Center, Faculty of Applied Science, University of Sri Jayewardenepura, Sri Lanka

HIGHLIGHTS

- Tri-metal composite incorporated polyacrylamide have developed for effective removal of fluoride, arsenate and chromate ions from aqueous media.
- The maximum adsorption capacities (q_{max}) of 43.85, 42.25 and 107.52 mg/g were achieved for arsenate, chromate and fluoride respectively at 300 K and in pH 7.00.

ARTICLE INFO

Article history:
Received 21 June 2018
Received in revised form 6 March 2019
Accepted 9 March 2019
Available online 14 March 2019

Keywords:
Tri-metallic composite
Adsorption
Arsenate
Chromate
Fluoride
Polyacrylamide
Removal
Isotherm
Kinetics

ABSTRACT

Excessive amounts of fluoride ions and other heavy metals in drinking water instigate a solemn threat to human health. Even though materials with specific binding ability towards these ions have been developed, it is yet a challenge to meet the practical utility of developing an efficient remedy as such. With this regard, a novel tri-metal composite incorporated polyacrylamide (TCIP) has developed. TCIP has shown a significant binding efficiency towards arsenate, chromate and fluoride ions in the presence of the other competing anions. The maximum adsorption capacities (q_{max}) of 43.85, 42.25 and 107.52 mg/g were achieved for arsenate, chromate and fluoride respectively at 300 K and in pH 7.00. Arsenate, chromate and fluoride adsorption is highly pH dependent. Monolayer adsorption of arsenate, chromate and fluoride ions was observed and adsorption data were found well behaved with the Langmuir adsorption isotherm. Arsenate, chromate and fluoride adsorption to TCIP has shown pseudo-second order adsorption kinetics, and no leaching of metal ions was observed from the metal composite into the aqueous medium.

1. Introduction

Water is indispensable to all of mankind. Regrettably, a sustainable supply of pure water for an affordable cost has become a challenge. It was assessed by the World Water Council that about 9 billion people will suffer from water scarcity in 2030 (Geise et al., 2010; Lee and Choi, 2002). Besides water shortage, polluted water has become a serious

* Corresponding author at: Department of Chemistry, University of Sri Jayewardenepura, Sri Lanka.
E-mail address: thilinidg@sjp.ac.lk (T.K. Mudiyanselage).

https://doi.org/10.1016/j.eti.2019.100353
2352-1864/

environmental problem in many parts of the world. Unfortunately, many people around the world are suffering from waterborne diseases. Among many hazardous toxins arsenic, chromate and fluoride could be highlighted as three major water pollutants.

Arsenic is a 20th most abundant element in the earth which exists as oxides or anion form (Mohan and Pittman, 2007). Natural weathering process, biological activity, agricultural pesticides, leaching of manmade arsenic compounds and anthropogenic activities have contributed to the increase of arsenic level in water (Mackenzie et al., 1979). The permissible limit for arsenic in drinking water is 0.01 mg/L as recommended by the World Health Organization (WHO) (Swarnkar and Tomar, 2012). The excess amount of arsenic in drinking water causes skin, lung and kidney cancers and chronic kidney disease (Matschullat, 2000).

Chromium is a well-known poisonous element. Major cradles of water pollution by chromium are glass industry, wood preservation, textile industry, metal cleaning, electroplating dyes and pigment processes industries (Sarin et al., 2006). The acceptable value of chromium in drinking water applauded by WHO is 0.05 mg/L (Mohan and Pittman, 2006). Among the variety of chromium ions, chromium (VI) is the most carcinogenic and mutagenic form (Matschullat, 2000).

Fluoride is an essential element for any living being because of its effects on strengthening bones, prevention of tooth decay and regulating growth rate etc. The excess amount of fluoride ions can cause dental fluorosis in children (>1 mg/L), skeletal fluorosis in adults (>4 mg/L) and crippling fluorosis (>10 mg/L) (Heller et al., 1997; Yu et al., 2015). Even though, the acceptable value of fluoride ions in drinking water is 1.5 mg/L, for tropical countries such as Sri Lanka upper limit values for fluoride ions in drinking water must be less than 1.0 mg/L (Mohapatra et al., 2009).

Many different techniques and methods (Akpomie et al., 2018) such as precipitation (Lee and Choi, 2002), using hydroxide based nano-materials (Li et al., 2018; Gu et al., 2018; Yu et al., 2018), metal oxide based materials (Li et al., 2018), oxidation reduction process (Nakano et al., 2001), coagulation (Emamjomeh and Sivakumar, 2009), adsorption (Mondal and George, 2015; Li et al., 2018) and ion-exchange (Dąbrowski et al., 2004) have been developed to remove arsenic, chromium and fluoride from aqueous media. Nevertheless, it is yet a challenge to develop a cost effective efficient technique for the removal of such carcinogenic pollutants.

Thus, the subject of this investigation is to introduce an efficient tri-metallic composite incorporated polyacrylamide hybrid as a remedy for the removal of arsenic, chromium and fluorides pollutants from aqueous media. The work reported here is a continuation of our previous endeavor on developing and characterizing the Fe–La–Ce tri-metallic composite (Thathsara et al., 2018). This work report the formulation, and characterization of the tri-metallic polyacrylamide hybrid material, and the efficiency of removing arsenic, chromium and fluoride ions from aqueous media. The absorption capacities, performances in co-existing ions, reusability, regeneration, adsorption kinetics and adsorption isotherms have been highlighted.

2. Materials and methods

2.1. Reagents and chemicals

All chemicals and reagents consumed in this work were of analytical grade and was purchased from Sigma Aldrich, Fluka and British Chemical House (BDH). $LaCl_3{\cdot}7H_2O$, $FeSO_4{\cdot}7H_2O$, $Ce(SO_4)_2{\cdot}4H_2O$ and NaOH were used for the synthesis of tri-metallic composite. Acrylamide, Potassium Persulphate (KPS), Tetraethyl methylenediamine (TEMED) and N,N′-methylene bisacrylamide (NBIS) were used to prepare the polymer matrix. NaOH and HNO_3 solutions were used to adjust the pH of the solutions.

Standard fluoride solution of 10,000 mg/L was purchased from WTW. Fresh 1000 mg/L of stock solutions were used for all analysis. Na_2HAsO_4 and K_2CrO_4 were used to prepare the stock solutions for arsenate and chromate.

2.2. Synthesis of trimetallic composite embedded polyacrylamide gel

The Fe–La–Ce tri-metallic composite were prepared and characterized as reported elsewhere (Thathsara et al., 2018). A series of tri-metal polymer hybrid was synthesized through bulk polymerization by varying the cross linker concentration and different molar percentage of tri-metallic composite. Acrylamide (3 mol dm^{-3}), N,N′-methylene-bis-acrylamide (NBIS), potassium persulfate (KPS) (0.01% moles) and Fe–La–Ce tri-metal composite (10 wt%) were added to 20 mL of deionized water. The solution was stirred for 2 h for better dispersion. The catalyst TEMED (0.05 mL of 1 wt% solution) was added drop-wise to the solution. Polymerization was carried out at 28 °C for 2 h. The resulted tri-metal incorporated polyacrylamide gel was further kept at 28 °C for 24 h. The prepared gel was washed, dried at 60 °C for 2 h in an oven and sieved using a 1 mm sieve. Adsorption experiments were conducted at 28 °C and at pH of 7.

2.3. Characterization of trimetallic composite incorporated polyacrylamide (TCIP)

TCIP was characterized before and after exposing to chromate, arsenate and fluoride using Nicolet IS 10 Fourier Transformation Infra-Red (FTIR) instrument at 500–4000 cm^{-1} wavenumber range. X-ray Diffraction (XRD) was carried out using (Rigaku, Ultima IV instrument) Cu Kα radiation ($\lambda = 1.540$ Å) over 2θ angle of 2°–70° with a step size of 0.02° to determine the crystallinity of prepared polymeric material and the incorporation of the tri-metal. The surface morphology

of TCIP was characterized before and after exposing to chromate, arsenate and fluoride using Hitachi SU6600 Analytical Variable Pressure FE-SEM (Scanning Electron Microscope) with an acceleration voltage of 15.0 kV. Samples were coated with a thin layer of gold prior to analysis and observations were conducted in the secondary electron mode. Furthermore, SEM coupled with EDS (Energy Dispersive Spectrum) was used to analyze the composition of TCIP via Oxford instruments EDX with AZtec software. Thermal stability of TCIP was determined using TGA (TA Instrument- SDTQ600) and DSC analysis (TA Instruments- DSCQ200).

2.4. Batch sorption studies

Adsorption experiments for arsenate and chromate were carried out in 250 mL of borosilicate stoppered conical flasks. For fluoride, 250 mL polypropylene plastic stoppered bottles were used. All the experiments were carried out at room temperature (28 ± 1 °C) using a mechanical shaker (Clifton shaker) and 100.00 mL portions of the test solution. Test solutions with a 10 mg/L of preliminary concentration were used to investigate the effect of pH on adsorption. The effect of ionic strength on the adsorption of arsenate, chromate and fluoride was determined by varying the concentration of NaCl in the medium. Residual concentration of arsenate, chromate and fluoride were measured after 3 h. Arsenate and chromate adsorption studies were carried with a 0.5 g/L amount of the adsorbent while fluoride studies were carried out with a 0.2 g/L dose of adsorbent. Sample pH was adjusted with either 1 M HNO_3 or NaOH. 10 mg/L test solution with adsorbent was placed on a shaker for (0–360) min to analyze optimum shaking time of chromate, arsenate and fluoride respectively. NaCl, $NaNO_3$, Na_2SO_4 and $NaHCO_3$ were used to analyze the influence of competitive ions on adsorption. The arsenate and chromate concentrations were determined by Atomic Adsorption Spectroscopy (AAS) using Thermo Scientific iCE 3000 series AAS. Fluoride concentrations were determined by a fluoride selective electrode (WTW F800) assisted with a multi-ion meter (WTW pH/ion 340i). Electrode was calibrated using a WTW 140,100 TISAB solution prior to use. Finally, the amount of arsenate, chromate and fluoride adsorbed per unit of adsorbate and removal efficiency were calculated using Eqs. (1) and (2) respectively.

$$q_e = \frac{(C_0 - C_e)}{m} \times v \tag{1}$$

$$\text{Removal efficiency } \% = \frac{C_0 - C_e}{C_0} \times 100\% \tag{2}$$

q_e (mg/g) — amount of adsorbate adsorbed per unit, m — the weight of the adsorbent, C_0 (mg/L) — initial concentration, C_e (mg/L) — concentration at equilibrium, V (L) — volume

2.5. The study of adsorption isotherms

A series of arsenate, chromate and fluoride solutions with initial concentrations in the range of 10.0 to 100.0 mg/L were prepared by adjusting the pH to 6.5. The amount of a 0.05 g of adsorbent dose for removal of metal ions (arsenate and chromate) and 0.02 g of tri-metal polymer hybrids were added into a flask containing 100 mL of arsenate, chromate and fluoride test solutions respectively and adsorption isotherms tests were carried out at 28 °C and 50 °C. The residual arsenate, chromate and fluoride concentration were analyzed using the method described previously in Section 2.4, while the Langmuir and Freundlich adsorption isotherms were analyzed using Eqs. (3) and (4) respectively (Dada et al., 2012).

$$\frac{C_e}{q_e} = \frac{1}{K_L q_{max}} + \frac{C_e}{q_{max}} \tag{3}$$

$$\ln q_e = \frac{1}{n} \ln C_e + \ln K_F \tag{4}$$

q_e — the weight of ions adsorbed per unit weight of adsorbent (in mg/g) at the equilibrium, C_e — the equilibrium concentration of ions (mg/L), K_L — the Langmuir constant, q_{max} — the maximum adsorption capacity of TCIP hybrid material for ions, K_F — the adsorption capacity and 1/n — the adsorption intensity.

2.6. The study of adsorption kinetics

Tri-metal incorporated polymer hybrid was shaken with 10 mg/L of 100 mL of arsenate, chromate and fluoride separately at 28 °C and pH of 6.0. Samples were taken out from the shaker at 60 min intervals. Finally, the residual concentration of arsenate, chromate and fluoride were analyzed using AAS and fluoride selective electrode connected to a multi-ion meter. The amount of arsenate, chromate and fluoride were calculated using Eq. (1). Pseudo first order rate model, Pseudo second order rate model and intra-particle diffusion rate model (Yang and Al-Duri 2005) were used to investigate the results.

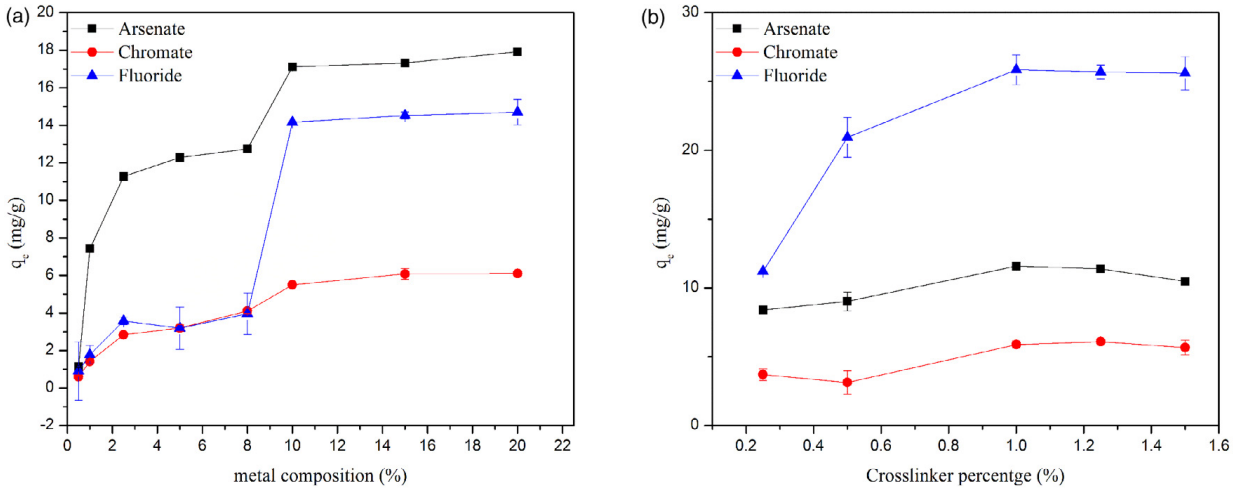

Fig. 1. (a) Variation of the adsorption capacity of TCIP on arsenate, chromate and fluorides with respect to different amounts of tri-metal percentages embedded, and Fig. 1(b) represents the variation of the adsorption capacity of TCIP on arsenate, chromate and fluorides with respect to different cross-linker percentages at 28 °C, pH 7.0, and at 3 M of monomer concentration.

2.7. Study the regeneration and reusability

The amount of 0.1 g of tri-metal polymer hybrid was added into 100 mL of 10 mg/L test solution and shaken for 2 h. The resulting adsorbent and supernatant were collected separately. Gathered adsorbent was introduce into 100 mL of 0.1M NaOH solution and it was shaken further for 2 h to regenerate the adsorbent. The mixture was separated again and the adsorbent was washed using deionized water. Washing cycles were repeated until pH become nearly neutral (7.0 ± 0.5). The produced adsorbent was dried at 333 K for 5 h. Residual concentration of arsenate, chromate and fluoride were measured using the method describe previously in Section 2.4. This process was repeated for three cycles to test the reusability of the tri-metal polymer hybrid.

All adsorption tests were triplicated to check precision among the results.

3. Results and discussion

3.1. Optimization of the synthesis of TCIP

The polymer, PAM was used as the matrix to imbed the tri-metal composite; thus the cross-linker density of the polymer and the amount of tri-metallic composite imbedded plays a major role on the efficacy of TCIP. The results of optimization of these two factors are highlighted in Fig. 1.

Rapid increase was observed on adsorption capacity of TCIP upon increasing the amount of tri-metallic composite up to the level of 10%. Even though further increment of tri-metallic composite increases adsorption, this increment is not that significant. Thus, 10% tri-metallic composition in TCIP was established for the study.

The cross-linker percentage of the polymer matrix will determine the porous structure of TCIP, which could subsidize the efficiency of TCIP in two different ways. Increasing the cross-linker percentages would entrap the tri-metallic composite steadily inside the polymer matrix, reducing the leachability of it. On the other hand, increasing cross-liker percentages would decrease the voids inside the matrix thus reducing the capillary pathways of ion diffusion which ultimately could affect the efficiency of TCIP negatively. Considering both factors, the amount of 1% cross-linker percentage was established for the study.

3.2. Characterization of trimetallic composite embedded polyacrylamide

3.2.1. Fourier Transform Infrared Spectroscopy (FTIR)

The FTIR spectrum (Supplementary Documents Fig. 1) of the TCIP clearly showed all the significant peaks of polyacrylamide (1103 cm^{-1} for C–C stretching vibration, 1325 cm^{-1} for CH_2 wagging vibration, 1454 cm^{-1} for –CN starching vibration, 1605 cm^{-1} for $-NH_2$ bending vibration, 1651 cm^{-1} for –CO stretching vibration, 2934 cm^{-1} for $-CONH_2$, C–C stretching vibration and the range of 3100–3500 cm^{-1} for $-NH_2$ and OH stretching vibration of trapped water) (Bhardwaj et al., 2008; Thakur et al., 2014). The corresponding peaks of the tri-metallic composite could clearly be seen at 3335 cm^{-1}, 1118 cm^{-1} and 1489 cm^{-1} due to the stretching vibration of OH^-, SO_4^{2-} and CO_3^{2-} respectively (Thathsara et al., 2018; Xiang et al., 2014). It can be clearly observed that the peaks of hydroxyl, sulfate and carbonate at 3333 cm^{-1}, 1103 cm^{-1} and 1454 cm^{-1} respectively, significantly have decreased after the adsorption of arsenate chromate and

fluoride. Additionally, the peak at 1454.89 cm^{-1} and 1325.33 cm^{-1} were shifted to 1409.31 cm^{-1} and 1352.10 cm^{-1} correspondingly, and after adsorption of arsenate onto the adsorbate the peak at 1103 cm^{-1} was shifted to 1115 cm^{-1} and 1119 cm^{-1} for chromate and fluoride adsorption respectively. Thus, results indicated that OH^{-}, SO_4^{2-} and CO_3^{2-} of tri-metallic composite were attributed to adsorption of these metals and fluorides onto the adsorbate. In addition, the FTIR spectra clearly shows that the peaks at 3333.94 cm^{-1}, 3189.26 cm^{-1}, 1651.72 cm^{-1} and 1605.40 cm^{-1} which correlates to symmetric and asymmetric $-NH_2$ and –C=O of polyacrylamide were significantly decreased after adsorption. It could be elucidated that lone electron pairs with polyacrylamide were also involved in adsorption of arsenate, chromate and fluoride. Furthermore, new peaks were formed at 835.06 cm^{-1}, 1048.65 cm^{-1}, and 864.95 cm^{-1} after the adsorption of arsenate, chromate and fluoride onto TCIP as shown in Fig. 1 (Supplementary Documents). This could be explained by the formation of new chelation bonds after the adsorption of these metals anions and fluorides onto TCIP. Conclusively, by comparing the FTIR spectra of TCIP before and after adsorption of ions, it clearly indicated that hydroxyl groups, sulfate groups, carbonates as well as the polymer matrix were engaged in the arsenate, chromate and fluoride absorption process of TCIP adsorbate.

3.2.2. Powder X-Ray Diffraction (PXRD)

XRD analysis was carried to establish the morphology of the TCIP and mainly to confirm the presence of the tri-metallic composite. The comparison of XRD patterns of the TCIP and after adsorption of each adsorbates are elaborately shown in Fig. 2 (Supplementary Documents). The characteristic peak in between 15° – 25° clearly confirmed that the TCIP has an amorphous polymer morphology. The pristine Fe–La–Ce tri-metal was reported to display significant peaks around 10.44°, 17.364°, 25.140°, 27.119°, 28.700°, 29.670°, 35.014°, 31.000° and 39.640° (Thathsara et al., 2018). The peaks at 10.44° and 27.119° were reported to correlated with $LaCe(CO_3)_3(H_2O)_8$ peaks. However, the peak at 10.44° has shifted to 10.36° while the peak at 27.119° has shifted to 27.19° on the developed TCIP due to the rearrangement of tri-metallic composite in polyacrylamide matrixes and formation of chelation bond between metal centers and electron donating groups.

Peaks at 18.54°, 22.54°, 29.43° and 34.56° were reported to correlate with $(H_3O)Fe^{3+}(SO_4)_2((OH)_6$. Despite the fact that peaks at around 17.364° shifted to 18.54°, 25.14° shifted to 22.54°, 29.670° shifted to 29.43° and 35.014° shifted to 34.56°, existence of $(H_3O)Fe^{3+}(SO_4)_2((OH)_6$ could be confirmed in TCIP.

Thus, most of the XRD diffraction lines of pristine tri-metallic composite reported could be clearly observed in XRD analysis of TCIP which confirmed the embedded tri-metallic composite. However, some diffraction lines are slightly altered or disappeared in the diffraction pattern of the TCIP due to the rearrangements of the packing of tri-metallic composite within the polyacrylamide matrix.

After the adsorption of metal ions and fluoride ions onto the TCIP, some major peaks (10.36°, 18.54° and 22.54°) became submerged in the broad peak of polyacrylamide.

3.2.3. Scanning Electron Microscopic Imaging (SEM)

SEM images of polyacrylamide polymer matrix, tri-metallic composite incorporated polyacrylamide, and the after adsorption of arsenate, chromate and fluoride onto TCIP, are shown in Fig. 2. The distinctive changes in the morphology of the TCIP adsorbent were noticeable when compared with polyacrylamide polymer matrix. The porous smooth surface of polyacrylamide surface has gained some roughness after the incorporation of tri-metallic composite into PAM. The porous structure and the heterogeneous nature of TCIP were clearly visible in Fig. 2(b) where uneven surface morphology and the availability of irregular assemblies were clearly being observed.

Sharp crystalline assemblies are notable on the SEM image of TCIP after adsorption of arsenate (Fig. 2(c)). When chromate and fluoride were adsorbed onto TCIP adsorbate, uneven assemblies on the adsorbent surface had been converted to sharp assemblies for chromate-TCIP (Fig. 2(d)) and for fluoride-TCIP (Fig. 2(e)). Nevertheless, the porosity of the polyacrylamide matrix has not been affected after the treatments.

3.2.4. The composition analysis using SEM-EDS

The SEM-EDS analysis for the PAM, TCIP and after adsorbed arsenate (TCIP-As), chromate (TCIP-Cr), and fluoride (TCIP-F) onto TCIP are tabulated in Table 1 (SEM-EDS data were taken using same polymer sites shown in Fig. 2). SEM-EDS analysis was used to study the adsorption process quantitatively. The mole percentage of Fe, La and Ce were approximately 1:1:1 in TCIP, TCIP-As, TCIP-Cr and TCIP-F. The careful composition of analysis confirms that there were no metal ions loss separately from the trimetal to the environment during adsorption; however some trimetal leach-out could be detected upon the adsorption of arsenate, chromate, and fluorides onto the TCIP. Mole percentage of 0.008% of arsenic and 0.096% of chromate were observed from TCIP after the ion treatments. The exact amount of fluoride adsorbed was unable to be quantified through SEM-EDS as F- Kα and the Fe- Kα are quite close in energy and thus they overlap in EDS analysis.

3.2.5. TGA And DTA analysis

The distinguished four steps were involved in weight loss of TCIP adsorbent (Plots are displayed in supplementary document in Fig. 3). The first step was due to the evaporation of physically bond water (moisture) which has the percentage amount of 15.78% in the range of 25–180 °C. The percentage amount of 12.19% in the temperature range of 230–340 °C correspond to the loss of lattice water and $-NH_2$ in the form of ammonia. The main weight-loss occurred at the third step which can be attributed to the scission of the C–C main chain of the poly acrylamide which has the highest percentage of weight lost (36.41%) (Van Dyke and Kasperski, 1993; Zhou and Wu, 2011).

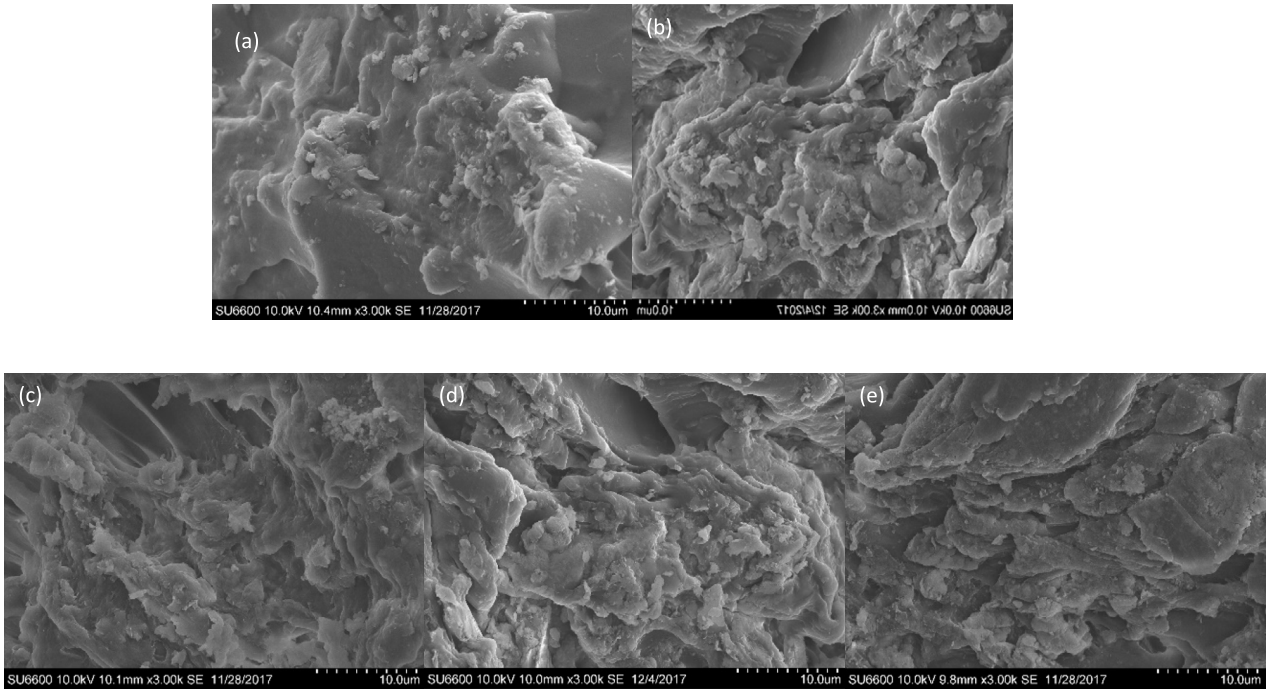

Fig. 2. SEM images for PAM (a), TCIP (b), after adsorption of arsenate (c), chromate (d) and fluoride onto TCIP (e).

Table 1
Elemental composition of the PAM, TCIP and after adsorbed arsenate (TCIP-As), chromate (TCIP-Cr) and fluoride (TCIP-F) onto TCIP.

Element	Mole percentage (%)				
	PAM	TCIP	TCIP-As	TCIP-Cr	TCIP-F
C	5.3333	5.3666	5.8500	5.6166	5.3583
O	1.6937	1.9187	1.6625	1.3125	1.5875
La		0.0151	0.0043	0.0172	0.0057
Ce		0.0121	0.0036	0.0264	0.0049
Fe		0.0107	0.0035	0.0340	0.0053
As			0.0080		
Cr				0.0096	

3.2.6. DSC analysis of TCIP

The DSC analysis of TCIP (Fig. 4 in supplementary documents) represents melting temperature (T_m), enthalpy and glass transition temperature (T_g). The glass transition temperature of TCIP was observed at 41.14 °C which is lower than the general T_g of polyacrylamide. The incorporation of trimetal has increased the amorphous nature of the polymer matrix. DSC spectrum highlights two significant peaks at 140.21 °C and 159.18 °C due to the melting of tri-metallic composite and polyacrylamide (Zhou and Wu, 2011).

3.2.7. Effect of contact time

Adsorption times of the three different ions were depicted in Fig. 3. Effective removal of arsenate and fluoride took 60 min to reach equilibrium while chromate consumed 120 min. There was no considerable change in the amount of arsenate, chromate and fluoride adsorbed per unit of adsorbate after 180 min. Initially the amounts of arsenate, chromate and fluoride removal efficiencies were rapid due to readily available binding sites, while later the rate was decreased due to the saturation of adsorbate on the free active sties.

3.2.8. Effect of pH and ionic strength

The pH of the medium plays a major role in adsorption of arsenate, chromate, and fluoride (Fig. 4). Below pH 2 was not reported for the adsorption of arsenate, as it showed low adsorption capacity due to the formation of H_2AsO_4 (Mohan and Pittman, 2007). The adsorption of arsenate onto TCIP was increased up to pH 5. At moderate pH values (2< pH <6.9), arsenate removal efficiency increases due to protonation of actives sites of TCIP. Therefore, the protonated TCIP attracts arsenate ions from aqueous media via electro statistic attraction. Above pH 6, TCIP deprotonated and formed anionic form of TICP which tends to form electro statistic repulsion in-between TCIP and arsenate and thus causes to decrease the efficiency of arsenate removal.

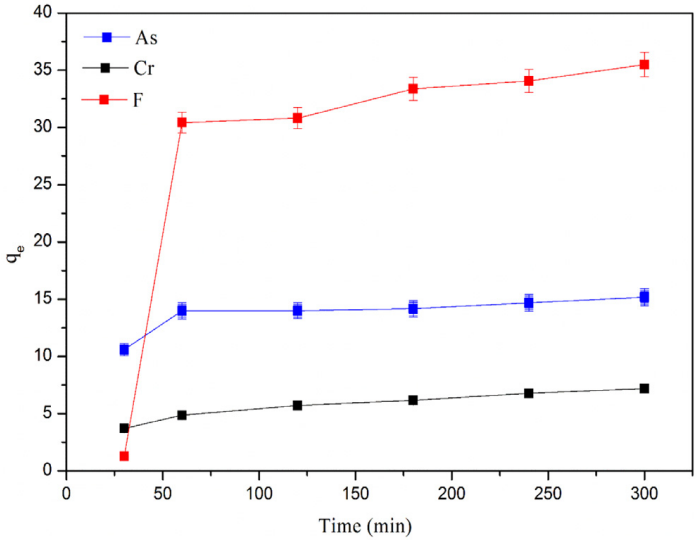

Fig. 3. The effect of contact time on arsenate (a), chromate (b) and fluoride (c) ions adsorption onto TCIP.

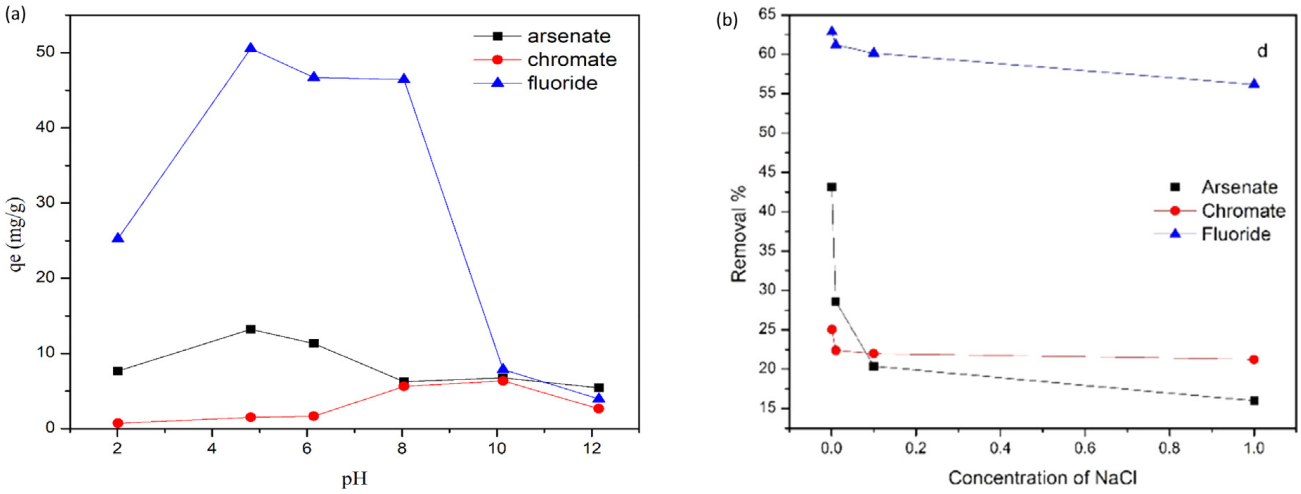

Fig. 4. The effect of pH on arsenate, chromate, and fluoride ions adsorption onto TCIP (a) and (b) effect of solution ionic strength.

Since H_2CrO_4 exist below pH 1, the amount of chromate ions adsorbed per unit of adsorbate is negligible. $HCrO_4^-$, CrO_4^{2-} and $Cr_2O_7^{2-}$ exists in between pH 2–6 (Miretzky and Cirelli, 2010). Therefore, the efficiency of ion removal was increased with increasing pH. The efficiency of chromate removal decreased at a higher pH (pH >10) due to the presence of large-numbered competitive OH^- ions which hinders the adsorption of chromate ions onto the TCIP.

The capacity of fluoride adsorption decreases considerably with increasing basicity of the medium as shown in Fig. 4c. The maximum adsorption capacity of 50.57 mg/g was achieved at pH 4.80. The maximum adsorption in acidic conditions is fortified by two hypotheses. Once the possible binding sites protonate in acidic media it may enhance the interactions between negatively charged fluoride ions with the positively charged binding sites (Biswas et al., 2009). The adsorption capacity of fluorides were significantly decreased below pH 4 due to the formation of HF (pKa 2.95) at strongly acidic conditions (Parashar et al., 2016). The interaction between positively charged binding sites of the adsorbent with hydrofluoric acid (HF) may not be that attractive. At very basic conditions, hydroxide ions compete with fluoride ions for active sites on the adsorbent, and consequently the adsorbent capacity is poor.

As shown in Fig. 4d, adsorption of arsenate, chromate and fluoride ions adsorption process were decreased upon addition of NaCl into the medium at pH 7.0. However, percentage removal was plateaued at NaCl concentration of 0.1 M. The electro statistic attraction between the novel TCIP and arsenate, fluoride and chromate ions are mainly involving in the removal process. In this system, an increase ionic strength has decreased the adsorption capacity. When the electro statistic attraction is repulsive, it may causes to decreased the adsorption process.

Table 2
Percent interference for arsenate, chromate and fluoride ions adsorbed onto adsorbate with presence in chloride, sulfate, nitrate and bicarbonate.

Pollutants	Percentage of interference (%)			
	Chloride	Sulfate	Nitrate	Bicarbonate
Arsenate	16.56	59.99	39.67	71.87
Chromate	41.82	97.21	15.24	51.74
Fluoride	3.64	16.71	2.34	95.65

3.2.9. Effect of interfering competitive ions

The effect of interfering anions for the arsenate, chromate, and fluoride adsorption by TCIP was studied (Table 2). The lowest intervention for arsenate, chromate and fluoride adsorption was observed from chlorides and nitrates, while a significantly high intervention was observed from carbonate ions. Sulfates ion interference for arsenate was modest; however, considerably high interference was shown towards chromate. Percentage interference of sulfate was considerably lower for fluorides comparing to arsenate and chromate adsorption process.

Percentage of interference from chloride, sulfate, nitrate and bicarbonate for arsenate, chromate and fluoride adsorbed onto the adsorbate were calculated using Eq. (5);

$$\%\mathrm{In} = \frac{q_{wo} - q_w}{q_{wo}} \times 100\% \tag{5}$$

%In = Percentage of interference
q_{wo} = adsorption capacity without interfering ions
q_w = adsorption capacity with interfering ions

3.3. Adsorption isotherms

The adsorption data were fitted to the Langmuir adsorption isotherm model and the corresponding regressions as a function of temperature are shown in supplementary documents of Figure 5 (28 °C, pH 7.00) and Figure 6 (50 °C, pH 7.00). Obtained regressions were with R^2 values over 0.99 for arsenate and chromate. Observation conforms that the adsorption is via formation of monolayer for arsenate and chromates. K_L decreased at higher temperature which implies the generation of imperfect monolayers on TCIP surface. At this stage ion exchange becomes the predominant mechanism for the arsenate and chromate adsorption process (Mohan and Karthikeyan, 1997). The K_L values (1.68 L/mg and 2.46 L/mg for arsenate and chromate respectively) were highest at 28 °C which indicates the best affinity of arsenate and chromate at room temperature (28 °C) whereas the K_L value (0.08 L/mg) for fluoride adsorption was highest at 50 °C which indicates the best affinity towards fluorides at 50 °C.

Arsenate, chromate and fluoride adsorption data for the TCIP, were also investigated using the Freundlich adsorption isotherm (Dada et al., 2012). According to the results, the process of fluoride adsorption was well fitted to Freundlich adsorption isotherms. As shown in Table 3, adsorption intensities ($1/n$) obtained for arsenate, chromate and fluoride adsorption data are less than 1, which implies that the adsorption sites of TCIP surface is heterogeneous in nature (Thathsara et al., 2018). Furthermore, it is clear that many active sites were involved in the arsenate, chromate and fluoride chelating process.

3.4. Adsorption kinetics

Adsorption kinetics studies lead to a better understanding of the adsorption process. Adsorption kinetics are investigated using the pseudo-first order rate model, pseudo-second order rate model, and the intra particle diffusion model (Gayani et al. (2017), and Reddad et al. (2002)). Kinetic equations assessed are given in Eqs. (6)–(8).

$$\log(q_e - q_t) = \log(q_e) - \frac{k_1}{2.303}t \tag{6}$$

$$\frac{t}{q_t} = \frac{1}{k_2 q_e^2} + \frac{1}{q_e}t \tag{7}$$

$$q_t = k_{id}t^{1/2} + C \tag{8}$$

q_t — the amount of ions removed at time t (mg/g), q_e — the adsorption capacity at equilibrium (mg/g), $k_{1,}$ – pseudo-first order rate constant, k_2 — pseudo-second order rate constant, k_{id} — intra particle diffusion rate constant, and C — a constant and was used to analyze the boundary layer effect.

Using Eq. (6), log (q_e – q_t) versus t was plotted to calculate the capacity for experimental adsorption of arsenate, chromate and fluoride (q_e) as 1.82 mg/g, 1.02 mg/g and 1.05 mg/g respectively, for the adsorption process. However, these values were significantly deviated from experimental values (Supplementary Figure 7(X) and Table 4). The regression

Table 3
Adsorption isotherms results for arsenate, chromate and fluoride adsorbed onto TCIP.

Isotherm model	Linear form of the equation	Isotherm parameters	
		Temperature/K	
		300	328
Langmuir isotherm model	$\frac{C_e}{q_e} = \frac{1}{K_L q_{max}} + \frac{C_e}{q_{max}}$	$HAsO_4^{2-}$ $q_{max} = 43.85$ mg/g $K_L = 1.6770$ L mg^{-1} $R^2 = 0.9947$ F^- $q_{max} = 107.52$ mg/g $K_L = 0.0759$ L mg^{-1} $R^2 = 0.9947$ CrO_4^{2-} $q_{max} = 42.24$ mg/g $K_L = 2.4570$ L mg^{-1} $R^2 = 0.9906$	$HAsO_4^{2-}$ $q_{max} = 49.26$ mg/g $K_L = 0.3845$ L mg^{-1} $R^2 = 0.9918$ F^- $q_{max} = 169.49$ mg/g $K_L = 0.0825$ L mg^{-1} $R^2 = 0.9854$ CrO_4^{2-} $q_{max} = 9.90$ mg/g $K_L = 0.3048$ L mg^{-1} $R^2 = 0.9631$
Freundlich isotherm model	$\ln q_e = \frac{1}{n} \ln C_e + \ln K_F$	$HAsO_4^{2-}$ $K_F = 37.89$ mg/g n = 28.49 $R^2 = 0.3959$ F^- $K_F = 25.99$ mg/g n = 3.3772 $R^2 = 0.9944$ CrO_4^{2-} $K_F = 36.58$ mg/g n = 24.5700 $R^2 = 0.6782$	$HAsO_4^{2-}$ $K_F = 31.74$ mg/g n = 9.59 $R^2 = 0.3992$ F^- $K_F = 27.67$ mg/g n = 2.961 $R^2 = 0.9894$ CrO_4^{2-} $K_F = 8.78$ mg/g n = 158.73 $R^2 = 0.0104$

coefficient of the plot was less than 0.96 and was also showing low linearity on arsenate, chromate and fluoride adsorption data to pseudo-first order kinetics. Thus, kinetic data was tested with pseudo-second order rate equation (Eq. (7)). As shown in Supplementary Figure 7(Y), the kinetic data is fitted perfectly well with the pseudo second order rate model with the regression coefficient value of over 0.99. This indicates that the adsorption process of arsenate, chromate and fluoride on TCIP surface perfectly follows pseudo second order kinetics (Zhao et al., 2018), and the rate-limiting step may be a process of chemisorption (Gad and El-Sayed, 2009).

When considering the results given in the plot in Supplementary Figure 7(Z), plot was linear (regression coefficient is 0.97) but has not passed the origin. Therefore, it can be concluded that the rate-limiting step for chromate adsorption may be chemisorption, or due to intra-particle diffusion. The plots in Supplementary Figure 7(X) and (Y) were not linear during the complete range of time (R^2 is 0.79 and 0.59 for arsenate and fluoride respectively). However, three unique linear segments (a, b and c) can be identified in the adsorption curve. Therefore, it can be concluded that intra-particle diffusion is not the only rate limiting step in the adsorption process of arsenate and fluoride onto TCIP (Ho and McKay, 1998). All the results drive to one conclusion which is that the adsorption process of TCIP accomplished with various processes. Adsorption process can be originated through external mass transfer while latter intra-particle diffusion may initiate. Thus, three probable key steps are: external mass transfer from the bulk solution, intra-particle diffusion, and adsorption of arsenate and fluoride onto TCIP. As the results of any ion do not pass through the origin, it can be determined that the above three proceedings do not arise simultaneously.

According to the adsorption isotherms results at 300 K, the predominant mechanisms for arsenate, chromate and fluoride adsorption is ion exchange with electro statistic attraction. When considering the kinetic results, the adsorption process of arsenate, chromate and fluoride on TCIP surface perfectly follows pseudo second order kinetics, and the rate-limiting step may be a process of chemisorption.

3.5. Feasibility of TCIP on natural water treatments

The feasibility of TCIP on natural water treatment was verified using five different natural water samples collected from five different regions in Sri Lanka. The collected fresh water samples were spiked with arsenate, chromate and fluoride ions because the initial concentrations of such ions were extremely low. The adsorption capacities of TCIP for arsenate, chromate, and fluoride are summarized in Table 5.

3.6. Regeneration ability and reusability of TCIP

It was observed that the ion adsorption process of TCIP is depend on the pH of the solution. Since adsorption decrease at higher pH (more than pH 10), by increasing the pH could release any adsorbed ions from the TCIP surface. Therefore,

Table 4
Kinetic model parameters for adsorption of arsenate, chromate and fluoride at 50 °C.

Kinetic model	Kinetic parameters		
	$HAsO_4^{2-}$	CrO_4^{2-}	F^-
Pseudo first order model	$k_1 = 4.60 \times 10^{-4}$ min^{-1} $q_e = 1.82$ mg g^{-1} $R^2 = 0.84$	$k_1 = 1.02$ min^{-1} $q_e = 1.02$ mg g^{-1} $R^2 = 0.96$	$k_1 = 6.90\times10^{-4}$ min^{-1} $q_e = 1.05$ mg g^{-1} $R^2 = 0.95$
Pseudo second order model	$k_2 = 5.09\times10^{-3}$ g mg^{-1} min^{-1} $q_e = 15.57$ g mg^{-1} $R^2 = 0.99$	$K_2 = 3.06\times10^{-3}$ min^{-1} $q_e = 7.96$ mg g^{-1} $R^2 = 0.99$	$K_2 = 1.39\times10^{-3}$ min^{-1} $q_e = 37.17$ mg g^{-1} $R^2 = 0.99$
Intra particle diffusion model	$K_{id} = 0.29$ mg g^{-1} min$^{-1/2}$ C = 10.29 mg g^{-1} $R^2 = 0.69$	$K_{id} = 0.27$ mg g^{-1} min$^{-1/2}$ C = 2.48 mg g^{-1} $R^2 = 0.98$	$K_{id} = 2.20$ mg g^{-1} min$^{-1/2}$ C = 1.69 mg g^{-1} $R^2 = 0.59$

Table 5
Ion removal efficiency of TCIP in natural water samples.

Sample no.	Initial concentration (mg/L)			pH	Initial conductivity (μS)	q_e (mg/g)		
	Arsenate	Chromate	Fluoride			Arsenate	Chromate	Fluoride
1	10.62	10.85	11.01	6.7	31.1	10.03	4.739	20.39
2	10.17	10.17	10.06	6.8	37.8	12.68	4.3644	16.08
3	9.99	10.99	10.73	7.9	37.7	12.15	4.7382	23.56
4	10.12	10.63	10.99	5.8	80.9	12.81	5.2676	14.89
5	11.02	9.99	10.15	8.1	40.2	15.39	5.0686	13.11

Table 6
Summary of regeneration ability for removal of fluoride ions at pH 10.

No. of regeneration cycle	Adsorption capacity (mg/g)			Percentage of desorption (%)		
	Arsenate	Chromate	Fluoride	Arsenate	Chromate	Fluoride
1	14.14	4.04	30.43	85.12	85.90	89.35
2	12.38	3.49	19.78	82.85	80.01	81.45
3	13.022	2.23	12.18	76.96	78.53	77.04

pH value increase to 10 using 1M NaOH to regenerate TCIP. Three cycles of adsorption and desorption process were studied and adsorption capacities and the percentage of desorption were shown in Table 6. Results confirm that, Fe–La–Ce tri-metallic composite exhibits good regeneration and reusability.

Conclusion

A novel TCIP hybrid material is presented as a remedy for the removal of arsenic, chromium and fluorides from aqueous media. Optimized polyacrylamide matrix consists of 1 mole% and 10 mole% cross linker and TC respectively. The maximum adsorption capacities (q_{max}) of 43.85, 42.25 and 107.52 mg/g were achieved for arsenate, chromate and fluoride respectively at 28 °C and in pH 7.0. However, the fluoride removal capacity of the pristine trimetal has been reduced by the incorporation into a polymer matrix. According to the FTIR spectra, it clearly indicates that both tri-metallic composite and polymer matrix are involved in the adsorption of arsenate, chromate and fluorides onto the adsorbate. SEM-EDS data reveals that after the adsorption process the mole percentage of Fe, La and Ce remains approximately at a 1:1:1 mole ratio in TCIP while it indicated the impossibility to leach out the individual trimetals into the environment. However, NaCl, $NaNO_3$ have not shown any effect on the arsenate and chromate adsorption process while $NaHCO_3$ and Na_2SO_4 demine the arsenate, chromate and fluoride uptake during the adsorption process. The adsorption processes of arsenate, chromate, and fluoride were well behaved with the Langmuir adsorption isotherm with a regression coefficient (R^2) of 0.99 at both temperatures of 28 °C and 50 °C. The pseudo second order rate fitted well with 0.99 of R^2 to all three kinetics of ion adsorption. TCIP exhibited excellent regeneration and reusability while maintaining a high adsorption capacity.

Acknowledgments

Financial support was provided by the University Research Grants (ASP/01/RE/SCI/2015/31, ASP/06/RE/SCI/2014/06 and ASP/01/RE/SCI/2015/29) at the University of Sri Jayewardenepura, Sri Lanka. The Center for Advanced Material Research and Instrument Center of the Faculty of Applied Sciences, University of Sri Jayewardenepura have facilitated the instrumental analysis for this study.

Appendix A. Supplementary data

Supplementary material related to this article can be found online at https://doi.org/10.1016/j.eti.2019.100353.

References

Akpomie, K.G., Dawodu, F.A., Eze, S.I., Asegbeloyin, J.N., Ani, J.U., 2018. Heavy metal remediation from automobile effluent by thermally treated montmorillonite-rice husk composite. Trans. R Soc. S. Afr. 1–10.

Bhardwaj, P., Singh, S., Singh, V., Aggrawal, S., Mandal, U.K., 2008. Nanosize polyacrylamide/SiO2 composites by inverse microemulsion polymerization. Int. J. Polym. Mater. 57 (4), 404–416.

Biswas, K., Gupta, K., Ghosh, U.C., 2009. Adsorption of fluoride by hydrous iron (III)–tin (IV) bimetal mixed oxide from the aqueous solutions. Chem. Eng. J. 149 (1), 196–206.

Dada, A., Olalekan, A.P., Olatunya, A.M., Dada, O., 2012. Langmuir, Freundlich, Temkin and Dubinin–Radushkevich isotherms studies of equilibrium sorption of Zn2+ unto phosphoric acid modified rice husk. IOSR J. Appl. Chem. 3 (1), 38–45.

Dąbrowski, A., Hubicki, Z., Podkoscienly, P., 2004. Selective removal of the heavy metal ions from waters and industrial wastewaters by ion-exchange method. Chemosphere 56 (2), 91–106.

Emamjomeh, M.M., Sivakumar, M., 2009. Review of pollutants removed by electrocoagulation and electrocoagulation/flotation processes. J. Environ. Manag. 90 (5), 1663–1679.

Gad, H.M., El-Sayed, A.A., 2009. Activated carbon from agricultural by-products for the removal of rhodamine-B from aqueous solution. J. Hazard. Mater. 168 (2), 1070–1081.

Gayani, B., Perera, A., Kottegoda, N., 2017. Thermodynamic, equilibrium and kinetic studies of adsorption of rhodamine B onto activated bamboo carbon. Desal. Water Treat. 67, 271–283.

Geise, G.M., Lee, H.-S., Miller, D.J., Freeman, B.D., McGrath, J.E., 2010. Water purification by membranes: The role of polymer science. J. Polym. Sci. B 48 (15), 1685–1718.

Gu, P., Zhang, S., Li, X., Wang, X., Wen, T., Jehan, R., Alsaedi, A., Hayat, T., Wang, X., 2018. Recent advances in layered double hydroxide-based nanomaterials for the removal of radionuclides from aqueous solution. Environ. Pollut. 240, 493–505.

Heller, K.E., Stephen, A., Eklund, D.D.S., Brian, A., Burt, B.D.S., 1997. Dental caries and dental fluorosis at varying water fluoride concentrations. J. Public Health Dent. 57 (3), 136–143.

Ho, Y., McKay, G., 1998. A comparison of chemisorption kinetic models applied to pollutant removal on various sorbents. Process Saf. Environ. 76 (4), 332–340.

Lee, H., Choi, W., 2002. Photocatalytic oxidation of arsenite in TiO2 suspension: Kinetics and mechanisms. Environ. Sci. Technol. 36 (17), 3872–3878.

Li, J., wang, X., Zhao, G., Chen, C., Chai, Z., Alsaedi, A., Hayat, T., Wang, X., 2018. Metal–organic framework-based materials: Superior adsorbents for the capture of toxic and radioactive metal ions. Chem. Soc. Rev. 47 (7), 2322–2356.

Mackenzie, F.T., Lartzy, R.J., Paterson, V., 1979. Global trace metal cycles and predictions. Math. Geol. 11 (2), 99–142.

Matschullat, J., 2000. Arsenic in the geosphere—a review. Sci. Total Environ. 249 (1), 297–312.

Miretzky, P., Cirelli, A.F., 2010. Cr (VI) and Cr (III) removal from aqueous solution by raw and modified lignocellulosic materials: A review. J. Hazard. Mater. 180 (1), 1–19.

Mohan, S.V., Karthikeyan, J., 1997. Removal of lignin and tannin colour from aqueous solution by adsorption onto activated charcoal. Environ. Pollut. 97 (1), 183–187.

Mohan, D., Pittman, C.U., 2006. Activated carbons and low cost adsorbents for remediation of tri-and hexavalent chromium from water. J. Hazard. Mater. 137 (2), 762–811, ls.

Mohan, D., Pittman, C.U., 2007. Arsenic removal from water/wastewater using adsorbents—a critical review. J. Hazard. Mater. 142 (1), 1–53.

Mohapatra, M., Anand, S., Mishra, B.K., Giles, D.E., Singh, P., 2009. Review of fluoride removal from drinking water. J. Environ. Manag. 91 (1), 67–77.

Mondal, P., George, S., 2015. Removal of fluoride from drinking water using novel adsorbent magnesia-hydroxyapatite. Water Air Soil Pollut. 226 (8), 241.

Nakano, Y., Takeshita, K., Tsutsumi, T., 2001. Adsorption mechanism of hexavalent chromium by redox within condensed-tannin gel. Water Res. 35 (2), 496–500.

Parashar, K., Ballav, N., Debnath, S., Pillay, K., Malty, A., 2016. Rapid and efficient removal of fluoride ions from aqueous solution using a polypyrrole coated hydrous tin oxide nanocomposite. J. Colloid Interface Sci. 476, 103–118.

Reddad, Z., Gerente, C., Andres, Y., Cloirec, P.Le, 2002. Adsorption of several metal ions onto a low-cost biosorbent: Kinetic and equilibrium studies. Environ. Sci. Technol. 36 (9), 2067–2073.

Sarin, V., Singh, T.S., Pant, K.K., 2006. Thermodynamic and breakthrough column studies for the selective sorption of chromium from industrial effluent on activated eucalyptus bark. Bioresour. Technol. 97 (16), 1986–1993.

Swarnkar, V., Tomar, R., 2012. Use of surfactant-modified zeolites for arsenate removal from pollutant water. J. Dispers. Sci. Technol. 33 (6), 913–918.

Thakur, N., Kumar, S.A., Parab, H., Pandey, A.K., Bhatt, P., Kumar, S.D., Reddy, A.V.R., 2014. A fluoride ion selective Zr (IV)-poly (acrylamide) magnetic composite. RSC Adv. 4 (20), 10350–10357.

Thathsara, S.K.T., Cooray, P.L.A.T., Mudiyanselage, T.K., Kottegoda, N., Ratnaweera, D.R., 2018. A novel Fe-La-Ce tri-metallic composite for the removal of fluoride ions from aqueous media. J. Environ. Manag. 207, 387–395.

Van Dyke, J.D., Kasperski, K.L., 1993. Thermogravimetric study of polyacrylamide with evolved gas analysis. J. Polym. Sci. A 31 (7), 1807–182.

Xiang, W., Zhang, G., Zhang, Y., Tang, D., Wang, J., 2014. Synthesis and characterization of cotton-like Ca–Al–La composite as an adsorbent for fluoride removal. Chem. Eng. J. 250, 423–430.

Yu, S., Wang, X., Pang, H., Zhang, R., Song, W., Fu, D., Hayat, T., Wang, X., 2018. Boron nitride-based materials for the removal of pollutants from aqueous solutions: A review. Chem. Eng. J. 333, 343–360.

Yu, Y., Yu, L., Chen, P., 2015. Adsorption of fluoride by Fe–Mg–La triple-metal composite: Adsorbent preparation, illustration of performance and study of mechanisms. Chem. Eng. J. 262, 839–846.

Zhao, G., Huang, X., Tang, Z., Huang, Q., Niu, F., Wang, X.K., 2018. Polymer-based nanocomposites for heavy metal ions removal from aqueous solution: A review. Polym. Chem.-UK 9, 3562–3582.

Zhou, C., Wu, Q., 2011. A novel polyacrylamide nanocomposite hydrogel reinforced with natural chitosan nanofibers. Colloids Surf. B 84 (1), 155–162.